applied sciences

MDPI

Article

An Experimental Study on the Migration of Pb in the Groundwater Table Fluctuation Zone

Jihong Qu [1,2,*], Tiangang Yan [1,2], Yifeng Zhang [1,2], Yuepeng Li [1,2], Ran Tian [1,2], Wei Guo [1,2] and Jueyan Jiang [1,2]

[1] College of Geosciences and Engineering, North China University of Water Resources and Electric Power, Zhengzhou 450046, China; ytg@stu.ncwu.edu.cn (T.Y.); yyds1231110@163.com (Y.Z.); liyuepeng@ncwu.edu.cn (Y.L.); tianran0227@163.com (R.T.); gwmengyeah@163.com (W.G.); jiangjueyan@stu.ncwu.edu.cn (J.J.)

[2] Collaborative Innovation Center for Efficient Utilization of Water Resources, Zhengzhou 450046, China

* Correspondence: qujihong@ncwu.edu.cn; Tel.: +86-133-9370-9096

Abstract: As a result of fluctuations in the shallow groundwater table, hydrodynamic conditions change alongside environmental conditions and hydrogeochemical processes to affect pollutant migration. The study aimed to investigate the migration, adsorption, and desorption characteristics of Pb on fine, medium, and coarse sand in the water table fluctuation zone by using several laboratory methods, including the kinetic aspects of Pb^{2+} adsorption/desorption and water table fluctuation experiments. The results showed that the adsorption and desorption curves fit the Elovich equation well at a correlation coefficient above 0.9. In the adsorption and desorption kinetic experiments for fine, medium, and coarse sand collected and from the floodplain, the maximum adsorption capacity of Pb^{2+} was 2367 mg·kg^{-1}, 1848 mg·kg^{-1}, and 1544 mg·kg^{-1}, respectively. The maximum desorption capacity of Pb^{2+} was 29.18 mg·kg^{-1}, 62.38 mg·kg^{-1}, and 81.60 mg·kg^{-1}, respectively. In environments with pH greater than 4, the adsorption capacity was proportional to the pH, but the desorption capacity decreased as the pH increased in water. As the water table varied, the lowest pH occurred in the polluted medium we set initially. When the distance between the pollutants and sample solution grew further, pH increased, and the Pb^{2+} concentration decreased in the sample solution. In the column experiment of water table fluctuations on coarse sand, Pb^{2+} migrated nearly 5 cm upward from the original pollutant and migrated less than 10 cm downward from that. In our experiments on medium and fine sand, the upward and downward migration distances were <5 cm. The groundwater table fluctuations, pH variation, and Pb concentration currently influence the migration of Pb.

Keywords: kinetic adsorption and desorption; groundwater table fluctuations; Pb; migration; experimental study

check for updates

Citation: Qu, J.; Yan, T.; Zhang, Y.; Li, Y.; Tian, R.; Guo, W.; Jiang, J. An Experimental Study on the Migration of Pb in the Groundwater Table Fluctuation Zone. *Appl. Sci.* **2022**, *12*, 3870. https://doi.org/10.3390/app12083870

Academic Editor: Bing Bai

Received: 1 March 2022
Accepted: 10 April 2022
Published: 12 April 2022

Publisher's Note: MDPI stays neutral with regard to jurisdictional claims in published maps and institutional affiliations.

Copyright: © 2022 by the authors. Licensee MDPI, Basel, Switzerland. This article is an open access article distributed under the terms and conditions of the Creative Commons Attribution (CC BY) license (https://creativecommons.org/licenses/by/4.0/).

1. Introduction

As an essential water source, groundwater plays a significant role in supplying urban and rural residents with water. The water table fluctuates under natural and human factors, such as rainfall, evaporation, exploitation [1], and recharge [2]. The area between the highest and lowest groundwater table is referred to as the groundwater table fluctuation zone [3,4]. Water table fluctuations allow both saturated and unsaturated soil to alternate within the environment. These fluctuations cause significant changes in the biochemical characteristics of that zone [5], including the adsorption, desorption, and dilution of pollutants, which correspondingly alter the groundwater environment. The influence of water table fluctuations on pollutant migration and transformation has attracted the attention of scholars.

Current studies mainly focus on solute migration and transformation, such as nitrogen [6], organic matter [7], heavy metals [8–10], and groundwater quality [11] under water table fluctuations. Liu et al. studied the nitrate change law under water table rise

using a sandbox model experiment, finding that the water environment gradually changed into a state of relative reduction, and the lateral flow of the experiment was conducive to the migration of nitrate [12]. Liu et al. studied the variation in nitrate concentration for two water table fluctuation conditions (the water table stayed constant and varied by 20 cm/10 days) [13]. Tian et al. adopted an experimental simulation involving three kinds of groundwater tables and different surface runoff velocities to study nitrate change laws on solute migrates to the soil surface. Their results showed that the solute transport process shares an essential relationship with surface runoff velocity and the groundwater table [14]. Wang et al. simulated and verified the regularity of soil salt migration under water table fluctuations at different groundwater depths using a laboratory column experiment with homogenic medium. They assumed that the capillary pressure and temperature field variation caused by water table fluctuations significantly influence the migration of organic pollutants [15]. Wang et al. used the TMVOC model (a numerical simulator for three-phase non-isothermal flow of water, soil gas, and a multi-component mixture of volatile organic chemicals) to simulate how benzene, toluene, ethylbenzene, and o-xylene (BTEX) migrate in areas caused by steam extraction under natural attenuation and groundwater table fluctuations [16]. Oostorm et al. used a two-dimensional sandbox to study the distribution of pollutants migrating from their source into soil and groundwater under water table fluctuations. They observed that pollutants migrate with the infiltrated water flow and dissolve when the water table rises, increasing the pollutant concentration in the sample solution [17]. Bustos Medina et al. studied iron hydroxide blockage in wells and its effect on groundwater table fluctuations. This blockage affects indexes such as the water table, pH, EC (electrical conductivity), and DO (dissolved oxygen). By adopting hydrogeochemical simulations, Medina et al. determined the minerals' reaction mode, such as iron ions and manganese ions in the aquifer [18]. Li et al. explored the nitrogen transport law for fluctuations in different water tables using laboratory-based column experiments and numerical simulation. Their results showed that groundwater table fluctuations influence the variation of dissolved oxygen in the solution and decrease the nitrate and ammonium concentrations, which is conducive to removing ammonium [19]. Liu et al. employed a numerical model to predict changes in Beijing's groundwater table when the South–North Water Diversion Project was open. They also analyzed changes to the vadose zone and the impact of solid waste on the groundwater environment [20]. On account of the South–North Water Diversion Project, Cao et al. analyzed chemical quality predictions in the Baoding Plain for when the groundwater table rises using hydrogeochemical simulations [21].

Heavy metals (Pb) pose potential risks to the soil ecosystem and human health [22–24]. China and other nations have focused on soil pollution prevention and control plans and the study of Pb migration characteristics [25,26]. Domestic and foreign scholars have studied the adsorption, desorption, and migration of heavy metal pollutants such as Cu, Cr, and Zn in soil [27–30]. Nonetheless, there are few reports on the migration laws of heavy metals under groundwater table fluctuations. Therefore, in this article, technical methods, including adsorption and desorption tests, water table fluctuation experiments, etc., were used to analyze the distribution characteristics of Pb in the vadose and saturated zones under different typical media. Our methods help research the migration of Pb in the groundwater table fluctuation zone and provide theoretical support for heavy metal pollution treatments for soil and groundwater, remediation, and protection.

2. Materials and Methods

2.1. Sample Collection and Process

The sample medium used in our laboratory was collected from the floodplain of the Yellow River in Mengjin District, Luoyang City, Henan Province. The sampling location is scoured by the Yellow River all the year round. As a result, the soil medium is relatively clean, and the background concentration of Pb is small, which has little influence on the laboratory experiment. Laboratory experiments need to separate sand into coarse medium and fine medium. The sample sand was collected and processed using the Technical

Specification for Soil Environmental Monitoring's quarter method [31]. Then, the sample sand was dried and crushed in the laboratory. Finally, the sample was divided into three typical media, including coarse, medium, and fine sand in the pH range of 8.5–9.3 with an organic matter content range of 0.241–1.070 $g \cdot kg^{-1}$. The basic physical and chemical properties of the soil are shown in Table 1.

Table 1. Physical and chemical properties of soil.

Sample	Particle Size (mm)	pH	Organic Matter Content ($g \cdot kg^{-1}$)
Coarse sand	0.5–1.0	8.5	0.241
Medium sand	0.25–0.5	8.8	0.587
Fine sand	0.125–0.25	9.3	1.070

2.2. Experimental Equipment

The following devices were employed for the adsorption and desorption kinetic aspects of Pb^{2+}: a digital water bath oscillator, high-speed desktop centrifuge, and microwave.

The experimental devices for water table fluctuations include a 90 cm long column, water tank with 25 L volume, peristaltic pump with 100 rpm speed, piezometer tube, and soil solution sampler. We set eight openings for sampling in every column at heights of 20, 30, 35, 40, 45, 50, 55, and 60 cm. The experimental devices are shown in Figure 1.

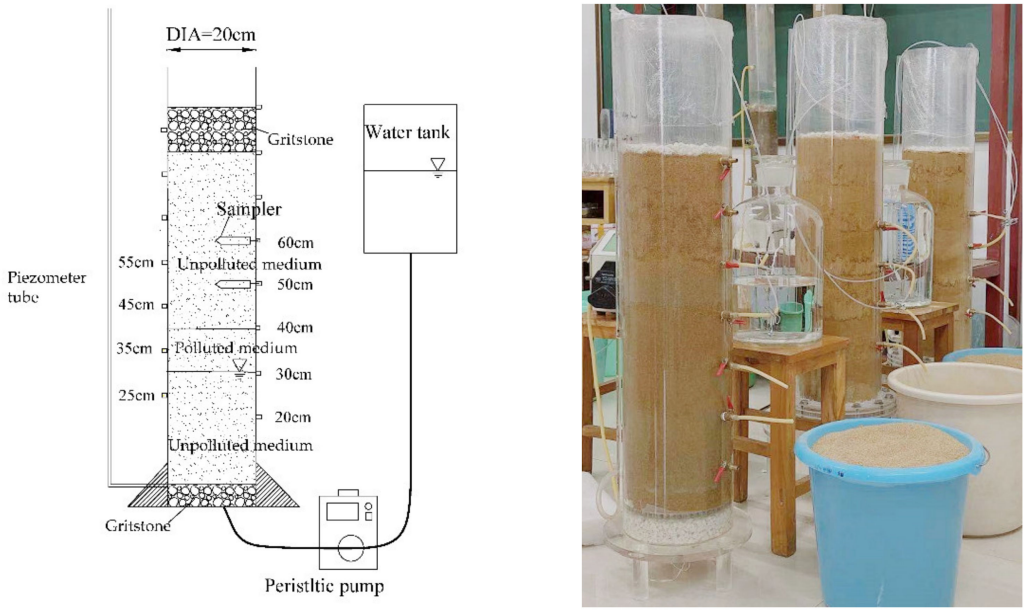

Figure 1. Experimental devices for the water table fluctuations. (**a**) The schematic diagram. (**b**) The field experiment diagram.

2.3. Experimental Methods

2.3.1. Adsorption and Desorption Experimental Methods of Pb

In this work, we completed the adsorption and desorption experiments, including the adsorption kinetics experiment, the desorption kinetics experiment, and the Pb adsorption and desorption quantities due to pH variation, in the laboratory. The experimental principle for adsorption was as follows: For the experiment, 50 mL of a 200 $mg \cdot L^{-1}$ $Pb(NO_3)_2$ solution was prepared mixing sample sand (the sample sand was divided into coarse, medium, and fine sand). After mingling, the supernatant liquids, which were samples obtained in 5, 10, 15, 20, 30, 60, 90, 120, 180, 240, 360, 480, 720, and 1440 min, passed through the oscillator for centrifugal filtration. The experimental principle for desorption was as follows. The desorption process resembles the first step of the adsorption process, i.e., the pollutant was

mixed with the sand medium. After shaking this mixture for 24 h, the filtered samples were passed through centrifugal filtration. Then, 50 mL of a 0.01 mg·L^{-1} $NaNO_3$ solution appended the filtered samples. The desorption time was the same as the adsorption time. The supernatant liquids were left behind by the oscillator via centrifugal filtration. The adsorption experiment at pH range of 4 to 6 and desorption experiment at pH range of 4 to 9 were as follows: Combining 50 mL of 500 mg·L^{-1} $Pb(NO_3)_2$ solution with 10 g of sample sand, the pH of the background solution was adjusted to target values, such as pH 4, 5, 6, with either HCl or NaOH. When reaching the equilibrium (1440 min), the supernatant liquids and residue for adsorption were obtained through centrifugal filtration. The residue was obtained at the end of the experiment on the adsorption due to pH variation. The solutions at pH 4, 5, 6, 7, 8, 9 were added to the residue. Then the mixture was shaken using oscillator (200 rpm·min^{-1}), the supernatant liquids for desorption were obtained through centrifugal filtration. The following equations reveal the calculation formulae for the adsorption and desorption capacities [32]:

$$Q_{ads} = \frac{V(C_1 - C_2)}{M} \quad (1)$$

$$Q_{des} = \frac{VC_3}{M} \quad (2)$$

where Q_{ads} is the adsorption capacity for the medium (mg·kg^{-1}), Q_{des} is the desorption capacity for the medium (mg·kg^{-1}), V is the supernatant volume (mL), C_1 is the original concentration for adsorption aspect (mg·L^{-1}), C_2 is the supernatant concentration for adsorption aspect (mg·L^{-1}), M is the mass of the sand sample (g), C_3 is the supernatant concentration for desorption aspect (mg·L^{-1}).

2.3.2. Experimental Methods for Water Table Fluctuations

The columns were filled with sand collected and processed from the field, including coarse, medium, and fine sand. The column was filled with gritstone around the 5 cm length, unpolluted medium around the 30 cm length, polluted medium around the 10 cm length, unpolluted medium around the 40 cm length, and gritstone around the 10 cm length, respectively, from bottom to top. A $Pb(NO_3)_2$ solution was mixed with the sample sand to produce 2000 mg·kg^{-1} contaminated mixture. After loading, the deionized water at pH 7 flowed up from the base of the column, whose pressure tube was used to measure the water table. The peristaltic pump controlled the water table variation, rising or falling. The initial water table was set in the column at the beginning of the experiment at about 20 cm high. Then, the water table was adjusted to increase 10 cm per day until it had continuously risen to 60 cm by adjusting the peristaltic pump. The same method was applied to the water table decrease, which decreased 10 cm per day until it reached a height of 20 cm. This process represented the completion of one water table fluctuation cycle. In the column for water table fluctuations, two cycles were continuously conducted. Figure 2 shows how the water table varies with time. In order to further understand the migration process of Pb in the medium under water table fluctuations, the Pb^{2+} concentration adsorbed in the medium was measured by digestion treatment after the experiment. The sampling medium was obtained from the 20–60 cm height at an interval of 5 cm.

2.3.3. Experimental Test Instrument

According to the groundwater quality standard (GB/T 14848-2017) and other standards, the Pb concentrations for the sample solution and sample sand were detected by a flame atomic adsorption spectrophotometer (FAAS, Manufacturer: Beijing Ruili Analytical Instrument Co. Ltd., Beijing, China). The pH of the solution was detected using the glass electrode method (Micro600, Manufacturer: Palintest Co. Ltd., Newcastle, UK). The medium sample was digested under microwave irradiation. The Pb contents were determined by FAAS.

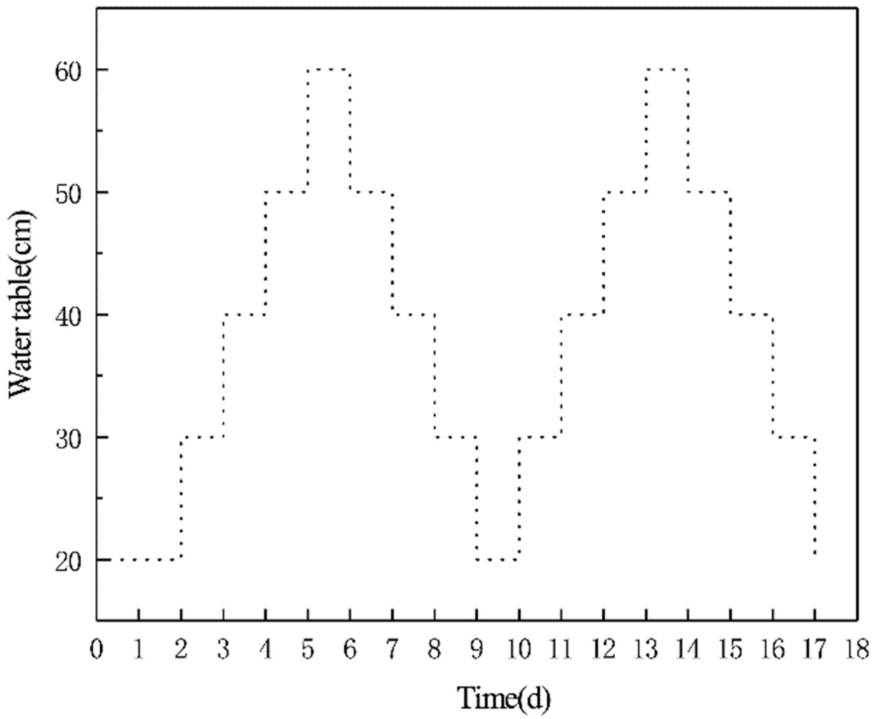

Figure 2. Water table fluctuations process.

3. Results and Discussion

3.1. The Curve of Adsorption and Desorption Kinetics

Figure 3 shows the curves of adsorption and desorption kinetics of Pb. The adsorption and desorption capacities of Pb^{2+} in the three sand media were significantly dissimilar. The adsorption and desorption quantity reached equilibrium in 1440 min. The maximum adsorption capacity of fine sand, medium sand, and coarse sand were 2366.6 $mg \cdot kg^{-1}$, 1847.6 $mg \cdot kg^{-1}$, and 1543.8 $mg \cdot kg^{-1}$, respectively. The maximum desorption capacity of coarse sand, medium sand, and fine sand were 81.6 $mg \cdot kg^{-1}$, 62.38 $mg \cdot kg^{-1}$, and 29.18 $mg \cdot kg^{-1}$, respectively. Compared to the hyperbolic diffusion model, pseudo-second-order model and Weber–Morris model, the data fit well to the Elovich model against various time ranges because the minimum R^2 value was 0.90. The fitting parameters are shown in Table 2. Based on the adsorption kinetics experiment data, Pb^{2+} in the contaminated solution was adsorbed rapidly onto the sampling sand within 240 min. The adsorption quantity gradually was stable from 240 to 1440 min in the experiment; this implies several points that adsorbed Pb^{2+} quickly on the medium surface at the initial stage. The effective points that adsorb Pb^{2+} gradually decreased with increasing reaction time, which gradually weakened the adsorption capacity until it reached equilibrium. The experiment's result aligned with the study of Ren, L. [33]. The same conditions occurred in the desorption kinetics experiment.

Figure 4 illustrates the effects of pH on the adsorption and desorption of sand medium. The adsorption capacity of Pb^{2+} in three sand media gradually increased at pH range of 4 to 6. The desorption capacity gradually decreased with increasing pH and the desorption quantity steadily approached equilibrium when the pH was between 8 and 9. Fine sand's adsorption and desorption capacities showed almost no change at different pH levels compared with medium and coarse sand. When the pH increased, the competitive adsorption sites of hydrogen ions in the medium decreased, and heavy metals mainly existed in the combined state of hydroxide or carbonic acid. This state is not conducive to their migration in the medium and increases adsorption capacity. These experimental conclusions are consistent with the literature [30,34].

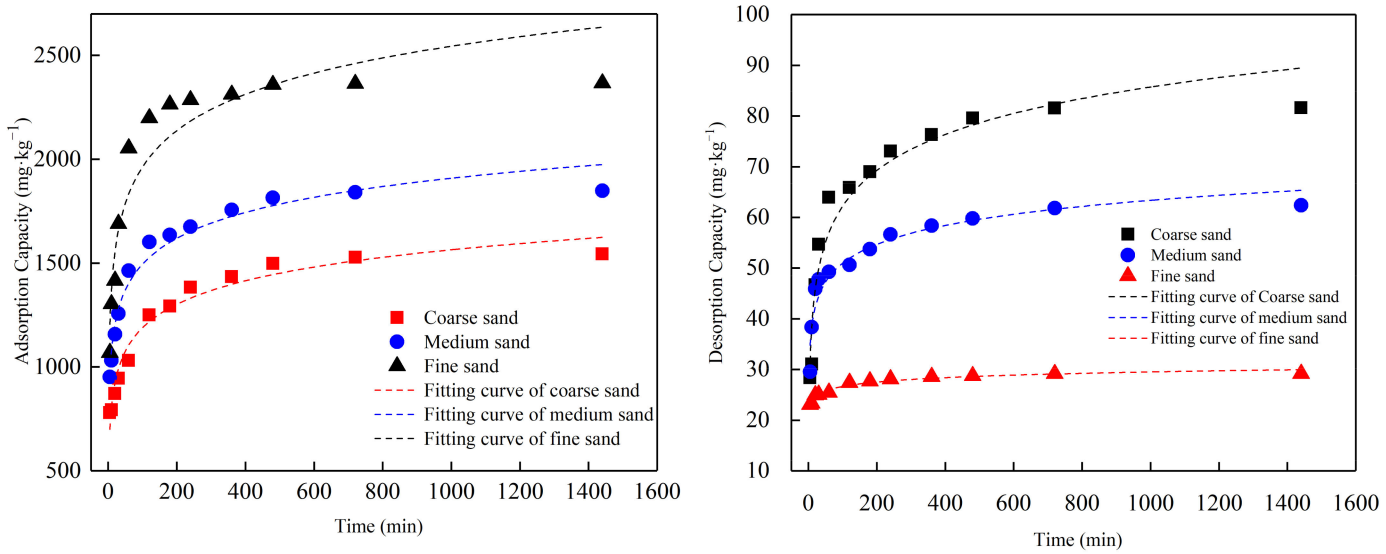

Figure 3. Curves of adsorption and desorption kinetics of Pb in different media: (**a**) the adsorption quantity variation of Pb based on adsorption kinetics; (**b**) the desorption quantity variation of Pb based on desorption kinetics.

Table 2. Kinetic parameters for adsorption and desorption of Pb in different media.

Category	Media	Elovich Equation			Hyperbolic Diffusion Equation			Pseudo-Second-Order Equation		Weber–Morris Equation		
		a_1	b_1	R^2	a_2	b_2	R^2	k_1	R^2	k_2	c	R^2
adsorption	Coarse sand	437.20	163.15	0.96	0.5513	0.0159	0.81	0.00005	0.72	24.52	851.0	0.81
	Medium sand	667.04	179.76	0.97	0.6171	0.0140	0.74	0.00006	0.83	25.81	1139.9	0.74
	Fine sand	799.14	252.62	0.90	0.6326	0.0143	0.60	0.00005	0.95	33.89	1497.1	0.60
desorption	Coarse sand	15.18	10.21	0.94	0.5208	0.0176	0.69	0.0008	0.96	1.43	42.50	0.69
	Medium sand	26.14	5.39	0.94	0.6465	0.0124	0.72	0.0022	0.81	0.77	40.33	0.72
	Fine sand	21.00	1.24	0.97	0.8298	0.0062	0.76	0.0165	0.55	0.18	24.21	0.76

Note: The data were fitted to the Elovich equation: $Q = a_1 + b_1 \ln t$, the hyperbolic diffusion equation: $Q/Q_{max} = a_2 + b_2\, t^{1/2}$, the pseudo-second-order equation: $Q = k_1\, Q_{max}{}^2\, t/(1 + k_1\, Q_{max}\, t)$ and the Weber–Morris equation: $Q = k_2\, t^{1/2} + c$, respectively, where Q is the adsorption/desorption capacity; t is time; a_1 and a_2 refer to constant associated with maximum adsorption/desorption amount for the Elovich equation and the pseudo-second-order equation, respectively, b_1 and b_2 refer to adsorption/desorption rate coefficient, k_1 and k_2 refer to adsorption/desorption rate coefficient for pseudo-second-order model and Weber–Morris model, respectively, c is constants related to the medium for Weber–Morris model, Q_{max} refers the equilibrium adsorption/desorption capacity for coarse sand, medium sand and fine medium.

3.2. pH Variation of Sample Solution on Water Table Fluctuation Zone

In Section 3.1, pH is one of the major factors affecting the adsorption and desorption capacities of Pb. Figure 5 illustrates pH variation at different sampling port heights in the water table fluctuation experiment on three typical media. The average pH variation at different sampling port heights is shown in Figure 6. The vertical direction of the column shows the distribution properties of pH in the sample solution. Firstly, pH decreased and then increased from the top to the bottom. The lowest pH often occurred at the height of 35 cm (pH = 4.7), where the location of original pollutants was consistent. The average pH of the three typical media followed the sequence of fine sand > medium sand > coarse sand. The aforementioned changes may be attributed to the increasing groundwater table since Pb^{2+} was not only adsorbed by the adsorption sites on the surface of soil particles, but also possibly combined with OH^- ions to obtain $Pb(OH)_2$ precipitation. Consequently, the concentration of OH^- ions decreased, so that the pH decreased in the solution, which resulted in a higher pH the further the distance. As the water table rose, the Pb^{2+} in the

solution was absorbed to saturation by the medium. A pH range from 4.5 to 7.5 was detected in the sample solution by coarse sand, at pH range from 5.1 to 7.8 by medium sand, and a pH range from 7.1 to 7.7 by fine sand. A comparison of the average pH values for the three typical media revealed that pH at different grain diameters generally followed the order of: coarse sand > medium sand > fine sand.

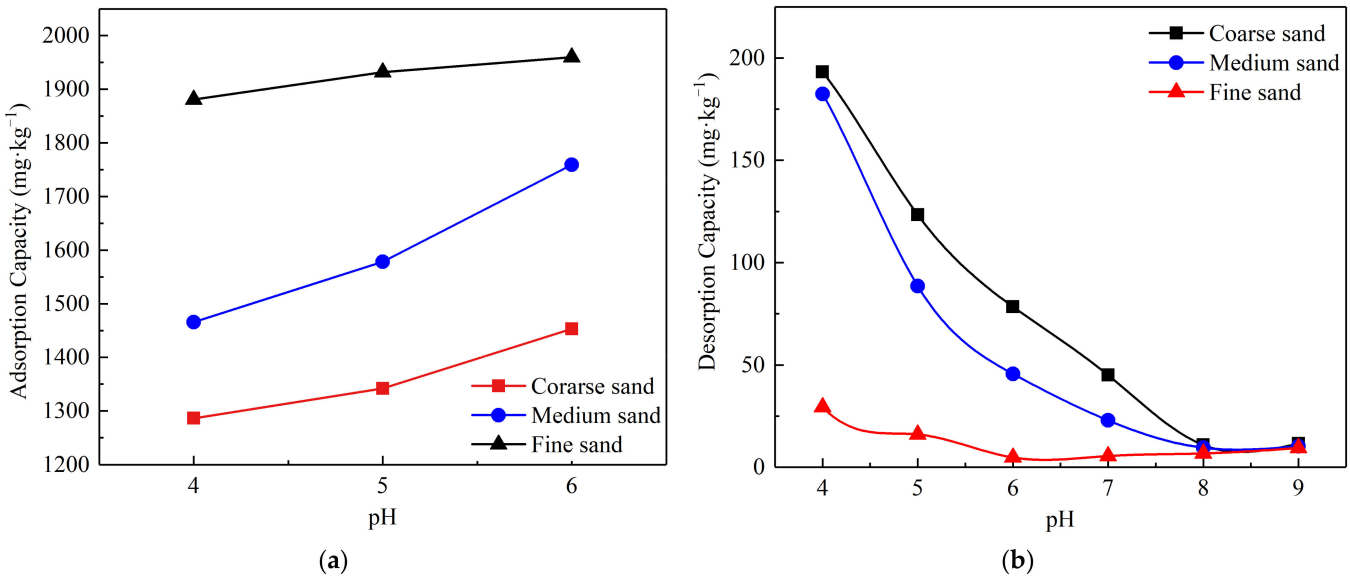

Figure 4. Effects of pH on adsorption (**a**) and desorption (**b**) on different media, including coarse, medium, and fine sand.

3.3. Migration Law of Pb Due to Water Table Fluctuations

Due to the strong adsorption capacity of fine sand, the migration ability of Pb in fine sand is weak. The Pb of each sample solution in the columns did not reach the instrument's detection limit (the instrument's detection limit (TAS-990A) is 0.01 mg/L). Therefore, we only analyzed the migration law of Pb in coarse and medium sand in this article. During groundwater table fluctuations, the variation in Pb concentration at different sample solutions is shown in Figure 7a (coarse sand) and Figure 7b (medium sand). The results of how Pb concentration is altered with water table fluctuations are shown in Table 3 and can be used to study the migration of Pb when the water table rises and falls in the experiment. Our analysis is as follows. (1) In the sample solution, when the height was 30 cm high in coarse sand, the water table height increased from 20 to 40 cm, and Pb^{2+} concentration increased in the range of 8.29–42.42% in the early-stage relative to the initial concentration on the first day. Then, with the water table fluctuations, Pb^{2+} concentration decreased in the range of 37.12–94.34%. This concentration declined by 9.54% on average within 8 days. (2) At the height of 35 cm for sample solutions in coarse sand, Pb^{2+} concentration decreased in the range of 4.01–97.47% with water table fluctuations. This concentration decreased by 6.68% on average within 14 days. (3) At the height of 40 cm for the sample solution in coarse sand, the concentration declined by 5.54% on average within 12 days. (4) At the height of 45 cm for the sample solution, Pb^{2+} was absorbed by coarse sand after 4 days. (5) At the heights of 30 and 40 cm for the sample solution in medium sand, Pb^{2+} was only detected on the first day. Afterward, Pb^{2+} was completely absorbed by the medium. (6) At the 30 and 40 cm heights for the sample solution in medium sand, Pb^{2+} concentration decreased in the range of 24.26–100%. This concentration decreased by 7.57% on average until the water table fluctuated at between 50 and 60 cm.

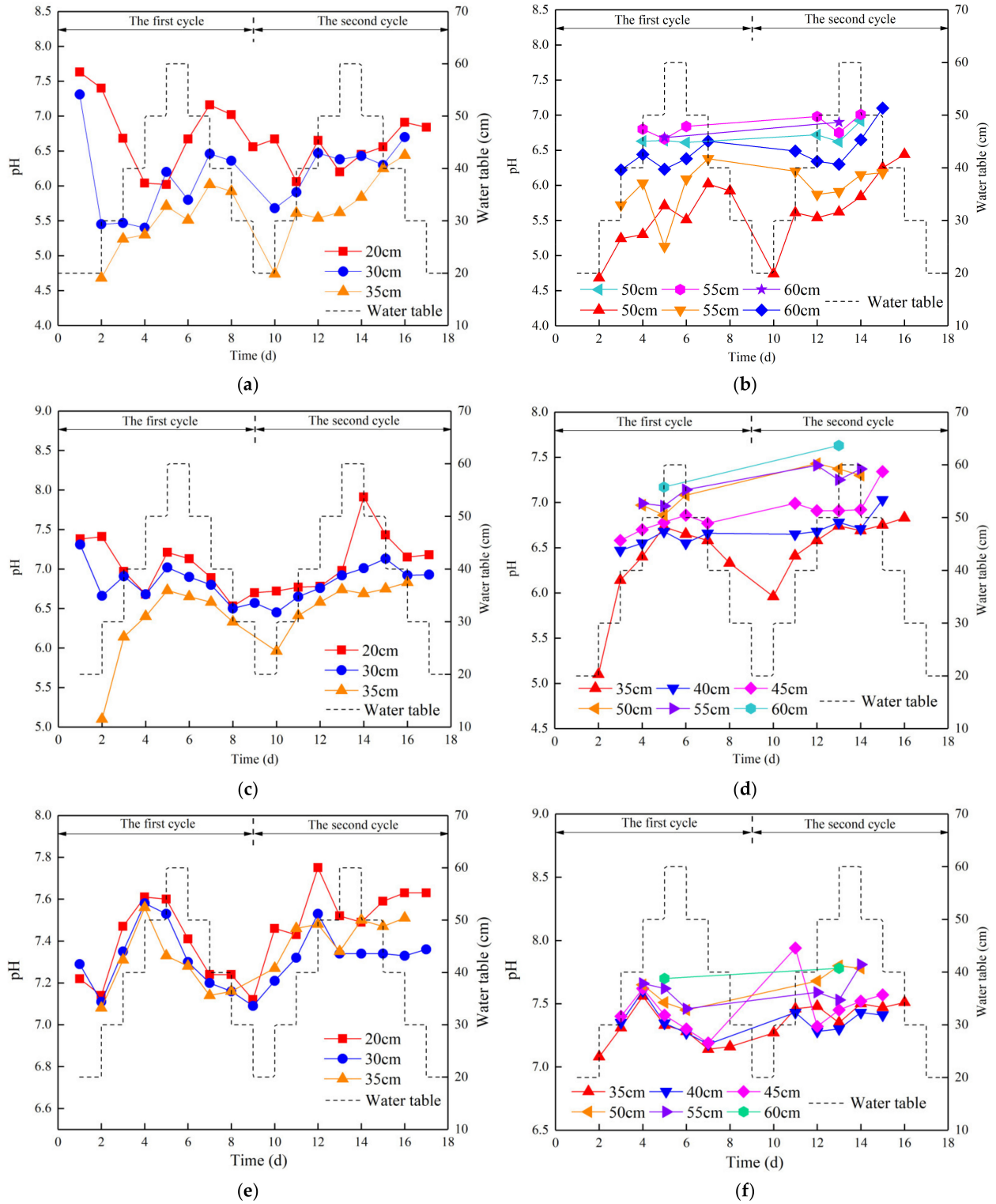

Figure 5. pH variation at different heights of sampling locations in the first and second cycles: (**a**) pH variation of coarse sand at sampling positions with heights of 20, 30, and 35 cm; (**b**) pH variation of coarse sand at sampling positions with heights of 35, 40, 45, 50, 55, and 60 cm; (**c**) pH variation of medium sand at sampling positions with heights of 20, 30, and 35 cm; (**d**) pH variation of medium sand at sampling positions with heights of 35, 40, 45, 50, 55, and 60 cm; (**e**) pH variation of fine sand at sampling positions with heights of 20, 30, and 35 cm; (**f**) pH variation of fine sand at sampling positions with heights of 35, 40, 45, 50, 55, and 60 cm.

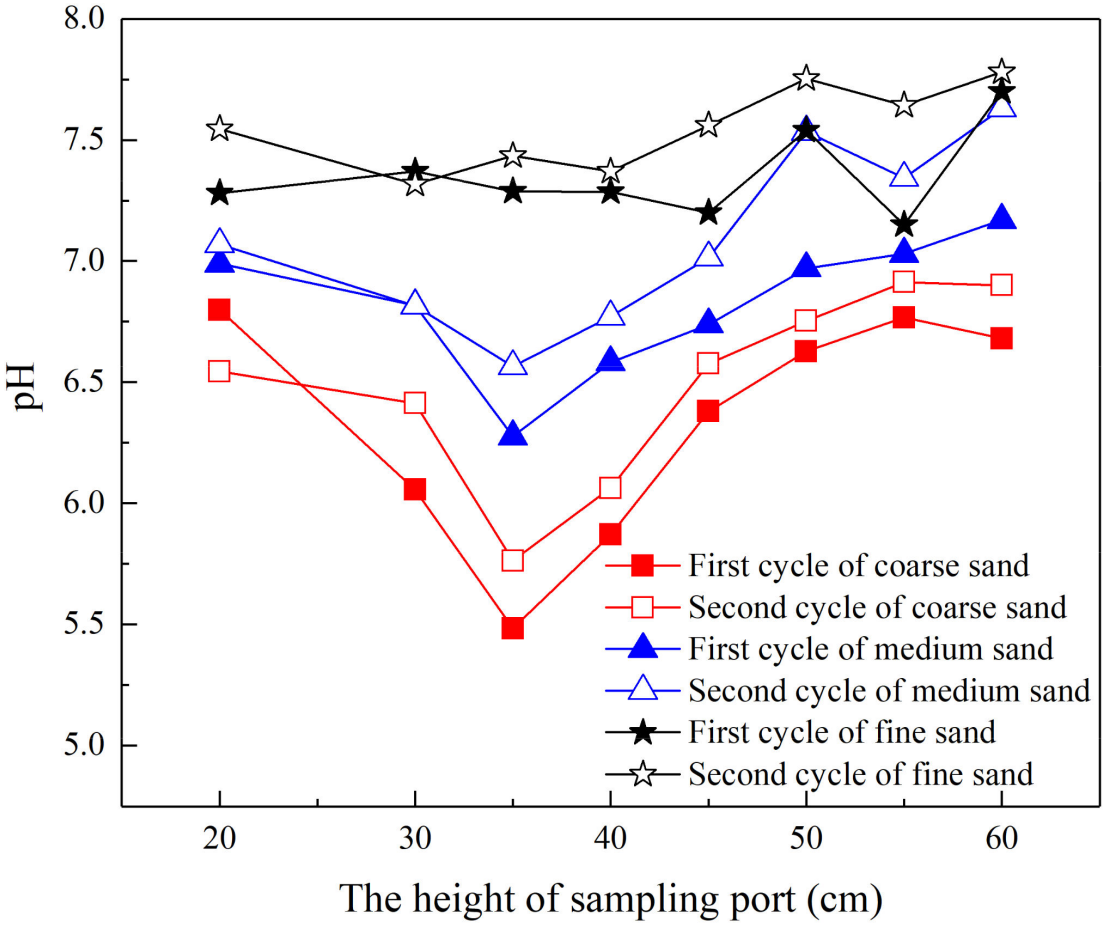

Figure 6. Average pH at different heights of sampling locations.

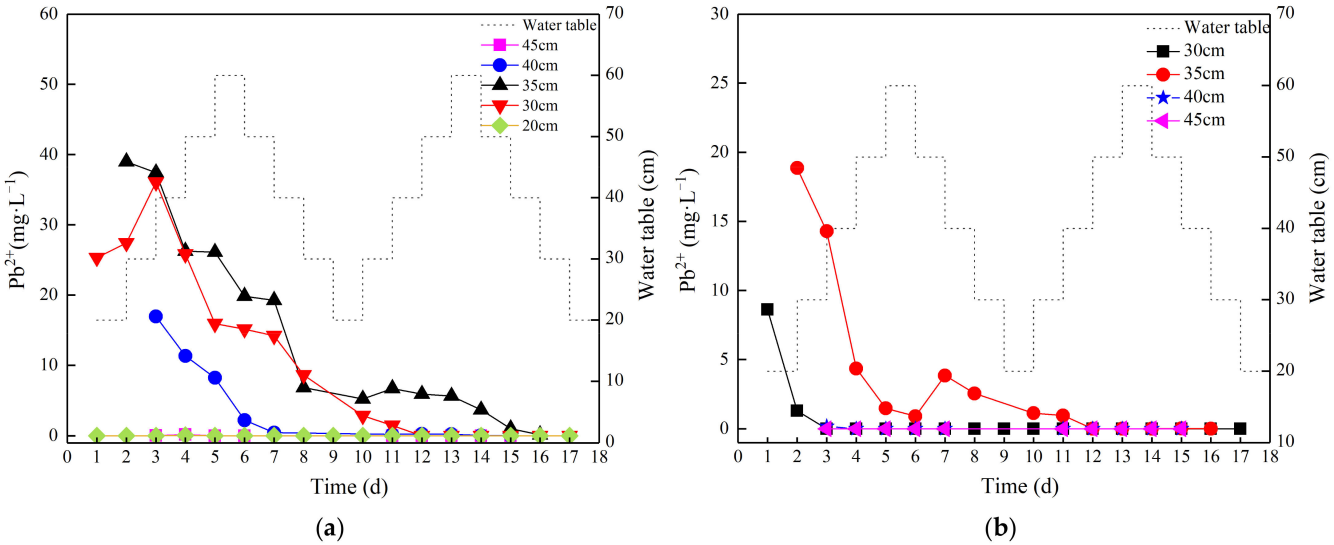

Figure 7. The Pb^{2+} concentrations vary in water table fluctuations. (**a**) The Pb^{2+} concentrations vary in columns filled with coarse sand; (**b**) the Pb^{2+} concentrations vary in columns filled with medium sand.

As seen in the analysis in Figure 5 of the pH and the water table, the closer the sample solution was to the pollutant in the rising water table, the lower the pH became, the greater the activity of Pb became, and the more desorption quantities resulted from polluted sand.

Therefore, at the height of 35 cm for the sample solution, Pb^{2+} concentration reached its maximum compared with the others. When the sample solutions were further away, the maximum concentration of Pb^{2+} was smaller. In a column of coarse sand, when the water table rose to 30 cm, the desorption quantity of Pb^{2+} reached its maximum, and the Pb^{2+} concentration in the solution reached its maximum. Throughout the whole experiment, the maximum concentration of Pb^{2+} at the 20, 30, 35, 40, and 45 cm sample solutions were 0.072, 36.061, 38.973, 16.941, and 0.042 mg·L^{-1}, respectively. Figure 7b shows that the adsorption capacity of medium sand is greater than that of coarse sand; therefore, the migration capacity of Pb^{2+} in medium sand becomes weak compared with that in coarse sand. Based on Figure 7b, Pb^{2+} is only detected at the heights of 30, 35, and 40 cm. In these sample solutions, the highest concentrations are 8.619, 18.862, and 0.164 mg·L^{-1}, respectively.

Table 3. Variation range of concentration of Pb in coarse and medium sand sampling ports with water table fluctuations.

Media	How Did the Water Table Fluctuate	Concentration Variation of Pb in the First Cycle (Compared with the Initial Concentration)				Concentration Variation of Pb in the Second Cycle (Compared with the Initial Concentration)			
		Sampling Port with Height of 40 cm	Sampling Port with Height of 35 cm	Sampling Port with Height of 40 cm	Sampling Port with Height of 45 cm	Sampling Port with Height of 30 cm	Sampling Port with Height of 35 cm	Sampling Port with Height of 40 cm	Sampling Port with Height of 45 cm
Coarse sand	20→30 cm	8.29%	-	-	-	-	-	-	-
	30→40 cm	42.42%	−4.01%	-	-	−88.82%	−86.67%	-	-
	40→50 cm	2.00%	−32.66%	−33.14%	285.71%	−94.34%	−82.83%	−98.91%	-
	50→60 cm	−37.12%	−33.04%	−51.56%	−100.00%	-	−84.93%	−98.48%	-
	60→50 cm	−40.23%	−49.12%	−87.05%	-	-	−85.60%	−98.82%	-
	50→40 cm	−43.94%	−50.60%	−97.42%	-	-	−90.68%	−99.68%	-
	40→30 cm	−65.96%	−82.47%	-	-	-	−97.47%	-	-
	30→20 cm	-	-	-	-	-	-	-	-
Medium sand	20→30 cm	−85.09%	-	-	-	-	-	-	-
	30→40 cm	-	−24.26%	-	-	-	−94.05%	-	-
	40→50 cm	-	−76.93%	−100.00%	-	-	−94.94%	-	-
	50→60 cm	-	−92.21%	-	-	-	−100.00%	-	-
	60→50 cm	-	−95.21%	-	-	-	-	-	-
	50→40 cm	-	−79.59%	-	-	-	-	-	-
	40→30 cm	-	−86.50%	-	-	-	-	-	-

Note: During the whole experiment, the concentrations in the solution sample at each sampling port did not reach the detection limit for columns filled with fine sand because of the strong adsorption capacities of fine and medium sand; therefore, they are not listed in this table. The "-" in the table indicates that the water sample was not obtained due to water table fluctuation limitations.

The experimental results of groundwater fluctuation showed that the underground water table rose to a height of 30 cm in coarse and medium sand after coming into contact with pollutants. The capillary band rose when the moisture content of the medium increased at the height of 30 cm. Then, Pb^{2+} in the medium dissolved into water under the effect of desorption. Pb^{2+} in the solution was still detectable since the water table fluctuated rapidly and Pb^{2+} in the solution had not been fully adsorbed by the medium. Reasons for why the concentration of Pb^{2+} decreased as the water table rose are as follows. (1) Due to the alkaline soil, the solution's pH increased with the rising water table, resulting in OH^- and Pb^{2+} combining in the water to form precipitation. (2) The adsorption quantity of the unpolluted medium was stronger than that of the pollution medium. The rising of the water table brought about Pb^{2+} adsorption one more time. (3) The adsorption and desorption of Pb is affected by hydrodynamic conditions. The change in hydrodynamic conditions caused Pb^{2+} to be desorbed and Pb^{2+} adsorbed by the medium. These two reactions were mutual until the adsorption equilibrium was reached.

3.4. Migration Characteristics of Pb in Soils with a Fluctuating Water Table

Figure 8 shows how the contents of Pb adsorbed by the sand sample varied at different heights. The maximum Pb content occurred at the height of 35 cm in three columns. Trace amounts of Pb were detected at the height range of 25–45 cm. The analyses in Figures 5

and 8 show that the maximum Pb content occurred where the minimum pH was detected. Therefore, the presence of heavy metal Pb decreases pH as a consequence of acidic soil. Zhai L et al. determined that precipitates and complexes may solidify the soil, causing grievous pollution to soils and crops [35].

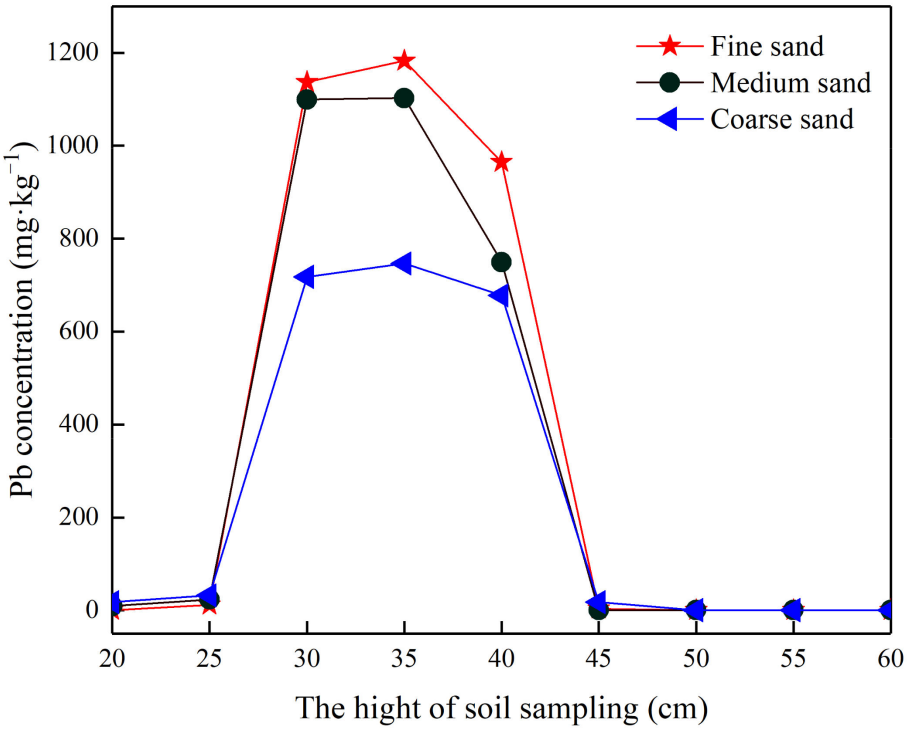

Figure 8. The variation of Pb concentration in the medium at different heights after experiments.

As the water table fluctuated, Pb^{2+} migrated upward or downward in the medium, but the migration distance of Pb^{2+} was more positively affected by the adsorption. The migration distance of Pb^{2+} in coarse sand was further than that in the medium sand or fine sand. The water table varied in coarse sand, the upward migration distance was only 5 cm high, and the downward migration distance was <10 cm high. In medium and fine sand, the upward and downward migration distance height was <5 cm.

4. Conclusions

- In the adsorption and desorption kinetic experiments for fine, medium, and coarse sand, the maximum adsorption capacity of Pb^{2+} was 2367 mg·kg^{-1}, 1848 mg·kg^{-1}, and 1544 mg·kg^{-1}, respectively. The maximum desorption capacity of Pb^{2+} was 29.18 mg·kg^{-1}, 62.38 mg·kg^{-1}, and 81.60 mg·kg^{-1}, respectively. For adsorption and adsorption experiments at different pH levels, the adsorption capacity of Pb^{2+} gradually increased and the desorption capacity gradually decreased with increasing pH in the sample solution at pH 4.0 and above. In these experiments, the desorption capacity held steady with an increase in pH from 8.0 to 9.0;
- In the water table fluctuation experiments, the pH detected in the sample solution varied with the water table fluctuation. The location was further away from the origin pollution we set, resulting in decreased pH in the sample solution. The minimum pH was consistent with the original pollution. At the same sample port, this universally followed the order of the medium's average pH: fine sand > medium sand > coarse sand. The Pb^{2+} concentration in the sample solution varies with time and water table fluctuations. Pb concentration in the medium results in Pb^{2+} forming desorption products in the solution that adsorb the experimental medium surfaces once again;

- The migration of Pb^{2+} is affected by pH in the solution, water table fluctuations, and the adsorption capacity of the medium. Water table fluctuations affect the desorption of Pb in the polluted medium. Consequently, the Pb^{2+} concentration in the solution changes. Then, the pH variation results in the adsorption and desorption capacities of Pb^{2+} changing as well;
- The effects of Pb's migration on groundwater table fluctuation zones are due to various factors. In this article, we only considered the water table, pH, and adsorption and desorption capacities in our analysis, which are the deficiencies of this work. Other meaningful factors will be added for future studies, such as dissolved oxygen, redox potential, etc.

Author Contributions: Conceptualization, J.Q.; methodology, T.Y.; validation, Y.Z.; formal analysis, Y.L.; investigation, R.T.; resources, W.G.; data curation, J.J.; writing—original draft preparation, J.Q.; writing—review and editing, J.Q. and T.Y.; funding acquisition, J.Q. All authors have read and agreed to the published version of the manuscript.

Funding: This research was funded by the Key R&D and Promotion Projects in Henan Province (202102310012), the Doctoral Research Fund of North China University of Water Resources and Electric Power (40651), and the Key Project of Science and Technology Research of Henan Education Department (14A170006).

Institutional Review Board Statement: Not applicable.

Informed Consent Statement: Not applicable.

Data Availability Statement: Data are contained within the article.

Conflicts of Interest: The authors declare no conflict of interest.

References

1. Li, W.; Wang, L.; Yang, H.; Zheng, Y.; Cao, W.; Liu, K. The groundwater overexploitation status and countermeasure suggestions of the North China Plain. *China Water Resour.* **2020**, *13*, 26–30.
2. Zhang, C.; Duan, Q.; Yeh, P.J.F.; Pan, Y.; Gong, H.; Gong, W.; Di, Z.; Lei, X.; Liao, W.; Huang, Z.; et al. The Effectiveness of the South-to-North Water Diversion Middle Route Project on Water Delivery and Groundwater Recovery in North China Plain. *Water Resour. Res.* **2020**, *56*, 10. [CrossRef]
3. Liu, X.; Zuo, R.; Wang, J.; He, Z.; Li, Q. Advances in researches on ammonia, nitrite and nitrate on migration and transformation in the groundwater level fluctuation zone. *Hydrogeol. Eng. Geol.* **2021**, *48*, 27–36.
4. Mu, E.; Ou, Y.; Dong, S.; Yang, J. Summary of research progress on groundwater level management. *Ground Water* **2019**, *41*, 33–34.
5. Rezanezhad, F.; Couture, R.M.; Kovac, R.; O Connell, D.; Van Cappellen, P. Water table fluctuations and soil biogeochemistry: An experimental approach using an automated soil column system. *J. Hydrol.* **2014**, *509*, 245–256. [CrossRef]
6. Zhang, D.; Cui, R.; Fu, B.; Yang, Y.; Wang, P.; Mao, Y.; Chen, A.; Lei, B. Shallow groundwater table fluctuations affect bacterial communities and nitrogen functional genes along the soil profile in a vegetable field. *Appl. Soil Ecol.* **2020**, *146*, 103368. [CrossRef]
7. Liu, Y.; Ding, A.; Liu, B.; Liang, X.; Li, S.; Zhang, L.; Yin, H. A review of the petroleum hydrocarbon contamination transformation performance in the zone of intermittent saturation. *Sci. Technol. Eng.* **2018**, *18*, 172–178.
8. Wu, Z.; Liu, G.; Qian, J.; Wei, Y.; Yue, Q. Experimental Study on the Vertical Migration of Pb from the Saturated Zone to Unsaturated Zone. *Environ. Sci. Technol.* **2019**, *42*, 36–41.
9. Rezaei, A.; Hassani, H.; Hassani, S.; Jabbari, N.; Fard Mousavi, S.B.; Rezaei, A. Evaluation of Groundwater Quality and Heavy Metal Pollution Indices in Bazman Basin, Southeastern Iran. *Groundw. Sustain. Dev.* **2019**, *9*, 100245. [CrossRef]
10. Rezaei, A.; Hassani, H.; Tziritis, E.; Fard Mousavi, S.B.; Jabbari, N. Hydrochemical characterization and evaluation of groundwater quality in Dalgan basin, SE Iran. *Groundw. Sustain. Dev.* **2020**, *10*, 100353. [CrossRef]
11. Yu, X. Groundwater Level Numerical Simulation Prediction and Its Environmental Influence Evaluation after the South-to-North Water Transferring Project. Master's Thesis, Jilin University, Changchun, China, 2004.
12. Liu, X.; Zuo, R.; Meng, L.; Li, P.; Li, Z.; He, Z.; Li, Q.; Wang, J. Study on the variation law of nitrate pollution during the rise of groundwater level. *China Environ. Sci.* **2021**, *41*, 232–238.
13. Liu, J.; Zhu, X.; Li, S.; Kang, L.; Ma, M.; Du, L. Effects of groundwater fluctuation on nitrate nitrogen transport after nitrogen application in cropland soil. *Chin. J. Eco-Agric.* **2021**, *29*, 154–162.
14. Tian, K.; Zhang, G.; Zheng, F. Chemical transport from soil into surface runoff under different ground-water tables. *J. Northwest A&F Univ.* **2009**, *37*, 193–200.
15. Wang, H.; Gao, W.; Ma, X. Research on the influence of groundwater level fluctuating on soil salin movement. *Sci. Technol. Innov. Her.* **2013**, *34*, 13–14.

16. Wang, Y.; Chen, L.; Yang, Y.; Li, J.; Tang, J.; Bai, S.; Feng, Y. Numerical simulation of BTEX migration in groundwater table fluctuation zone based on TMVOC. *Res. Environ. Sci.* **2020**, *33*, 634–642.
17. Oostrom, M.; Dane, J.H.; Wietsma, T.W. A review of multidimensional, multifluid, intermediate-scale experiments: Flow Behavior, Saturation Imaging, and Tracer Detection and Quantification. *Vadose Zone J.* **2007**, *6*, 610–637. [CrossRef]
18. Bustos Medina, D.A.; van den Berg, G.A.; van Breukelen, B.M.; Juhasz-Holterman, M.; Stuyfzand, P.J. Iron-hydroxide clogging of public supply wells receiving artificial recharge: Near-well and in-well hydrological and hydrochemical observations. *Hydrogeol. J.* **2013**, *21*, 1393–1412. [CrossRef]
19. Li, X.; Yang, T.; Bai, S.; Xi, B.; Zhu, X.; Yuan, Z.; Wei, Y.; Li, W. The effects of groundwater table fluctuation on nitrogen migration in aeration zone. *J. Agro-Environ. Sci.* **2013**, *32*, 2443–2450.
20. Liu, Y.; Sun, Y.; Yin, K. Prediction of groundwater environment in Beijing after water entering the capital by the South-north Water Diversion. *Hydrogeol. Eng. Geol.* **2005**, *05*, 93–96.
21. Cao, W.; Yang, H.; Gao, Y.; Nan, T.; Wang, Z.; Xu, S. Prediction of groundwater quality evolution in the Baoding Plain of the SNWDP benefited regions. *J. Hydraul. Eng.* **2020**, *51*, 924–935.
22. Cheng, X. Research progress of lead pollution on soil. *Ground Water* **2011**, *33*, 65–68.
23. Lee, J.; Son, Y.; Pratheeshkumar, P.; Shi, X. Oxidative stress and metal carcinogenesis. *Free Radic. Biol. Med.* **2012**, *53*, 742–757. [CrossRef] [PubMed]
24. Rezaei, A.; Hassani, H.; Fard Mousavi, S.B.; Jabbari, N. Evaluation of Heavy Metals Concentration in Jajarm Bauxite Deposit in Northeast of Iran Using Environmental Pollution Indices. *Malays. J. Geosci.* **2019**, *3*, 12–20. [CrossRef]
25. Shi, X.; Li, L.; Zhang, T. Water Pollution Control Action Plan, a Realistic and Pragmatic Plan—An Interpretation of Water Pollution Control Action Plan. *Environ. Prot. Sci.* **2015**, *41*, 1–3.
26. Ge, F.; Yun, J.; Xu, K.; Zhang, M.; Xu, L.; Li, Y.; Zhang, A. Progress of research on environmental criteria for lead in soil. *J. Ecol. Rural Environ.* **2019**, *35*, 1103–1110.
27. Singh, O.V.; Labana, S.; Pandey, G.; Budhiraja, R.; Jain, R.K. Phytoremediation: An overview of metallic ion decontamination from soil. *Appl. Microbiol. Biotechnol.* **2003**, *61*, 405–412. [CrossRef]
28. Singh, S.P.; Ma, L.Q.; Harris, W.G. Heavy Metal Interactions with Phosphatic Clay: Sorption and Desorption Behavior. *J. Environ. Qual.* **2001**, *30*, 1961–1968. [CrossRef]
29. Jacques, D.; Šimůnek, J.; Mallants, D.; van Genuchten, M.T. Modelling coupled water flow, solute transport and geochemical reactions affecting heavy metal migration in a podzol soil. *Geoderma* **2008**, *145*, 449–461. [CrossRef]
30. Zhang, R.; Yao, S.; Ao, Y. Vertical transport rules of Cu, Cd, Pb in the surface of soil. *J. Shanghai Jiaotong Univ. (Agric. Sci.)* **2013**, *31*, 67–71.
31. China National Environmental Monitoring Centre; Nanjing Environmental Monitoring Center Station. Technical Specification for Soil Environmental Monitoring (HJ/T 166-2004). Available online: http://www.mee.gov.cn/image20010518/5406.pdf (accessed on 9 December 2004).
32. Azouzi, R.; Charef, A.; Hamzaoui, A.H. Assessment of effect of pH, temperature and organic matter on zinc mobility in a hydromorphic soil. *Environ. Earth Sci.* **2015**, *74*, 2967–2980. [CrossRef]
33. Ren, L. Adsorption-Desorption Characteristics Research of Pb, Cr, Ni in Sediment and Soil. Master's Thesis, Jilin Agricultural University, Changchun, China, 2017.
34. Zheng, S. Studies on the Transformation and Transport of Heavy Metals in Typical Chinese Agricultural Soi. Master's Thesis, Zhejiang University, Hangzhou, China, 2010.
35. Zhai, L.; Chen, T.; Liao, X.; Yan, X.; Wang, L.; Xie, H. Pollution of agricultural soils resulting from a tailing spill at a Pb-Zn mine:A case study in HuanJiang Guangxi Province. *Acta Sci. Circumstantiae* **2008**, *6*, 1206–1211.